Glassy Dynamics of $Rb_{0.40}(ND_4)_{0.60}D_2PO_4$

Z. Kutnjak, C. Filipič, A. Levstik, and R. Pirc
Jožef Stefan Institute, University of Ljubljana, 61111 Ljubljana, Slovenia

(Received 23 December 1992)

The complex dielectric constant of $Rb_{0.40}(ND_4)_{0.60}D_2PO_4$ has been measured in the frequency interval from 1 mHz to 1 GHz at temperatures between 40 and 140 K. A novel frequency-temperature plot of the data is introduced to show that the behavior of the relaxation spectrum is reflected in the real part of the dielectric constant. It is found that the highest relaxation frequency $f_2 = 1/2\pi\tau_{\min}$ follows an Arrhenius behavior, whereas the lowest frequency $f_1 = 1/2\pi\tau_{\max}$ exhibits a critical decay according to the Vogel-Fulcher law $f_1 \propto \exp[-U/(T-T_0)]$ with $T_0 = 32.9$ K.

PACS numbers: 77.22.Gm, 64.70.Pf, 77.22.Ej, 77.90.+k

Mixed crystals $Rb_{1-x}(ND_4)_xD_2PO_4$ or their deuterated isomorphs (DRADP) exhibit in the intermediate concentration range $0.2 \leq x \leq 0.7$ the characteristics of a deuteron glass [1]. Specifically, a slow nonexponential relaxation of remanent polarization and a splitting between the zero-field-cooled and field-cooled dielectric susceptibilities have been observed below a characteristic temperature T_f [2]. The observed value of the freezing temperature T_f in DRADP depends on the experimental time scale, suggesting that the freezing process itself is a dynamic phenomenon. In common with other glassy systems, the relaxation process in DRADP is polydispersive and thus characterized by many time scales [1]. As one approaches the freezing transition in a spin glass, the maximum relaxation time is expected to diverge [3,4] according to the Vogel-Fulcher law with a critical temperature T_0. Clearly, the concept of an equilibrium transition temperature is meaningful on an infinite time scale only and thus the following two questions may be raised: (i) Can the static value of T_f be determined in a real experiment carried out on a finite—albeit long—time scale; (ii) how is the freezing temperature T_f related to the Vogel-Fulcher temperature T_0?

In this Letter we present a discussion of the above problems in the light of new experimental data for the dielectric relaxation in DRADP at $x = 0.60$. Earlier experiments performed on deuterated and undeuterated samples have indicated that the dynamic processes can be described within the so-called parallel relaxation picture, i.e., as an integral over a set of Debye-type exponential relaxations with a broad distribution of relaxation times [1,4,5]. Various attempts at determining the relaxation spectrum were described in the literature, such as using a symmetric Gaussian distribution [6], or a Fröhlich-type distribution with smooth edges [7]. By adopting a Vogel-Fulcher ansatz for the relaxation frequencies, Courtens has shown that the dielectric loss data in a broad frequency range can be mapped onto a single curve [1]. This Vogel-Fulcher scaling yields a critical temperature $T_0 = 30.3 \pm 0.7$ K for DRADP with $x = 0.62$, a value much lower than the freezing temperatures $T_f \approx 90$ K and $T_f \approx 60$ K estimated from model calculations [8] in connection with NMR [9] and field-cooling data [2], respectively, obtained on samples with comparable concentrations. This discrepancy clearly suggests the importance of time-scale effects in deuteron glasses.

The frequency-dependent complex dielectric constant $\varepsilon^*(\nu,T) = \varepsilon' - i\varepsilon''$ provides rather direct information on the dynamic processes occurring in deuteron glasses. In order to investigate the relaxation spectrum of DRADP, we have carried out an extensive experimental analysis of the dielectric relaxation along the tetragonal crystallographic *a* axis. A system with suitable concentration was chosen, namely, $x = 0.60$. The measurements were performed between 40 and 140 K on two samples cut from the same DRADP single crystal. The frequency range from 1 mHz to 1 GHz was covered by three different techniques: (a) The Sawyer-Tower bridge technique was used in the frequency range from 1 mHz to 1 Hz. The polarization charge was measured by means of an electrometer. A computer was used as a digital phase detector and the real and imaginary parts of a complex dielectric constant were extracted by the least-squares method. (b) The frequency dependence of the complex dielectric constant between 20 Hz and 1 MHz in the temperature interval 40 to 80 K was measured using a HP 4284A Precision LCR meter. Both techniques were used successively on the same platelet of DRADP with dimensions $1\times4\times5$ mm, in the temperature interval between 50 and 60 K. (c) Because of a steady increase of relaxation frequencies on increasing the temperature, the high frequency measurements from 1 MHz to 1 GHz above 68 K had to be performed by the HP 4191A RF Impedance Analyzer. In the temperature interval from 68 to 80 K the techniques (b) and (c) complemented each other. High frequency measurements were performed in separate runs from 68 to 140 K on a different platelet approximately 1 mm high and 7 mm in diameter, which was fixed at the center of a radial line, thus terminating the coaxial reflectometer. The temperature of the samples was monitored and stabilized to within ±0.1 K by an Oxford Instruments continuous flow cryostat. The dielectric constant was always determined on slowly cooling (≈ 1 K/min) the system.

In Fig. 1 a set of representative Cole-Cole diagrams are shown, where ε'' is plotted as a function of ε' at

0031-9007/93/70(25)/4015(4)$06.00

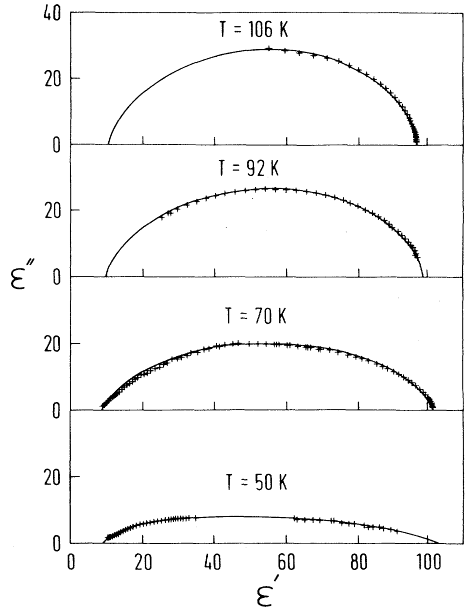

FIG. 1. Measured values of ε'' plotted vs ε' in DRADP ($x = 0.60$) at four temperatures, as indicated. Solid lines are fits obtained with a general multiparameter expression for the relaxation distribution.

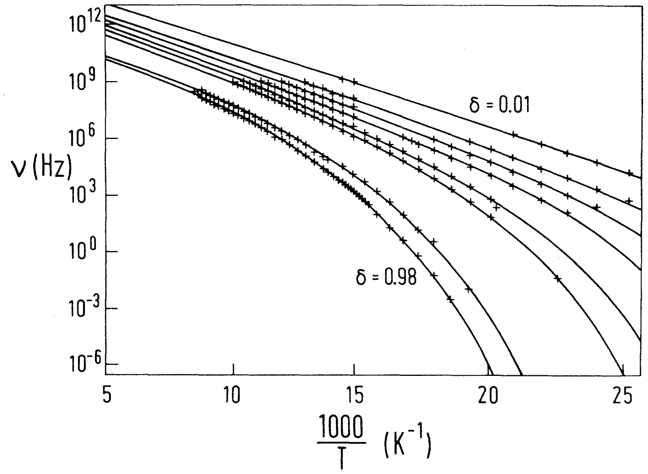

FIG. 2. Frequency-temperature plots of the data for several fixed values of the reduced dielectric constant δ. Top to bottom: $\delta = 0.01, 0.03, 0.06, 0.12, 0.23, 0.33, 0.89, 0.98$. The curves are fits obtained with a linear approximation Eq. (3) for the relaxation spectrum.

four different temperatures. The curves represent fits to a general expression of the type of Eq. (1) below, using a rather general form for the relaxation distribution function of $g(\ln f)$; however, we will not describe the details of this procedure here. At high temperatures, the frequency dependence of the complex dielectric constant $\varepsilon^*(\nu, T)$ shows a nearly monodispersive relaxation; however, at lower temperatures the dielectric relaxation in DRADP becomes strongly polydispersive [10].

To describe such complicated behavior uniquely in the entire temperature range, we represent the data for the real part of the complex dielectric constant $\varepsilon'(\nu, T)$ in the following way. First we express, as usual, $\varepsilon'(\nu, T)$ as a sum of Debye relaxations [1,10],

$$\frac{\varepsilon'(\nu, T) - \varepsilon_\infty}{\varepsilon_s - \varepsilon_\infty} = \int_{y_1}^{y_2} \frac{g(y)\,dy}{1 + (\nu/f_a)^2 \exp(-2y)}\,, \tag{1}$$

where $y = \ln(f/f_a)$ with $f = 1/2\pi\tau$ representing the relaxation and f_a an arbitrary attempt frequency, respectively, and $g(y)$ is the distribution of relaxation frequencies. We assume that $g(y)$ extends over a finite frequency interval $y_1 \leq y \leq y_2$.

Next, we introduce a new symbol for the reduced dielectric constant appearing in Eq. (1), i.e.,

$$\delta = \frac{\varepsilon' - \varepsilon_\infty}{\varepsilon_s - \varepsilon_\infty}\,. \tag{2}$$

The essential step now is to regard δ as an independent parameter. This implies that at any given temperature T a frequency ν must be found at which the prescribed value of δ—and therefore of ε'—is reached. As one scans ε' from ε_∞ to ε_s, the parameter δ varies from 0 to 1. In practice, this procedure may require an interpolation between the available discrete experimental points $\varepsilon'(\nu, T)$ in order to obtain a fixed value of δ, and hence the corresponding value of $\nu(T, \delta)$. The parameters ε_s and ε_∞ are actually known from the static and the high frequency data, respectively, and are thus independent of the distribution function $g(y)$. We will discuss this point in more detail later.

Focusing on Eq. (1), we realize that the frequency ν specifies the position of the frequency filter represented by the factor $1/[1 + (\nu/f_a)^2 \exp(-2y)]$ under the integral. Because of the steplike shape of this filter, which effectively opens in a unit frequency interval around $y \approx \ln(\nu/f_a)$, and since the distribution function $g(y)$ extends itself over many orders of magnitude in the frequency domain, we conclude that at low values of ε', i.e., δ close to 0, the relaxation processes arising from the high frequency part of the distribution function determine the value of the integral. In contrast, as $\delta \approx 1$, the whole relaxation spectrum contributes and the frequency filter probes the shape of $g(y)$ near its lower edge y_1.

To illustrate the above qualitative argument, we have plotted in Fig. 2 the frequencies $\nu(T, \delta)$ vs $1/T$ for a set of fixed values of δ. Ignoring for the moment the solid curves, it is obvious that the data corresponding to small values of δ show a nearly linear behavior. This, in turn, suggests an Arrhenius-type behavior for the relaxation frequencies near the high frequency edge of the distribution function. On the other hand, for $\delta \to 1$, the frequency ν falls off dramatically as the temperature is lowered. Such behavior is then indicative of a divergence of the lower edge y_1 of the distribution function.

To determine precisely the temperature dependence of the lower boundary of the relaxation spectrum, we now need a specific model for the distribution function $g(y)$. The solid curves in Fig. 2 are fits to a simple linear ansatz for the relaxation spectrum:

$$g(y) = 2(y - y_1)/(y_2 - y_1)^2, \qquad y_1 \le y \le y_2, \quad (3)$$

with $y = \ln(f/f_a)$, $y_1 = \ln(f_1/f_a)$, and $y_2 = \ln(f_2/f_a)$. Again, f is the relaxation frequency, while the fit parameters $f_1 = 1/2\pi\tau_{\max}$ and $f_2 = 1/2\pi\tau_{\min}$ represent the low and the high frequency edge, respectively, of the relaxation spectrum. In accordance with the qualitative arguments given above, we assume a Vogel-Fulcher temperature behavior for f_1, i.e.,

$$f_1 = f_{01}\exp[-U/(T - T_0)], \quad (4)$$

and similarly an Arrhenius-type behavior for f_2,

$$f_2 = f_{02}\exp(-E/T). \quad (5)$$

The solid curves in Fig. 2 are least-square fits by Eqs. (4) and (5), resulting in the following values for the parameters: $T_0 = 32.9 \pm 0.5$ K, $f_{01} = (5.5 \pm 2.0) \times 10^{11}$ Hz, $U = 770 \pm 70$ K, $f_{02} = (1.8 \pm 0.6) \times 10^{14}$ Hz, $E = 980 \pm 70$ K.

We have also tried to describe the critical divergence of the lower boundary of the relaxation spectrum with a more complicated ansatz [11]:

$$f_1 = f_{01}(T/T_0 - 1)^{\alpha}\exp[-U/(T - T_0)^{\beta}], \quad (6)$$

based on the theory of critical hierarchy [11,12]. It turns out that the divergent behavior of f_1 is practically the same as above. Namely, by fitting the parameters in Eq. (6) to the data in Fig. 2 we obtain $\alpha = 0.01 \pm 0.01$, $\beta = 0.97 \pm 0.03$, and $T_0 = 32.7 \pm 0.5$ K. Thus the simpler relation (4) adequately describes the critical divergence of the lower edge of the relaxation spectrum.

It should be noted that the linear shape of $g(y)$ has been chosen in order to describe the low frequency cutoff of the relaxation spectrum and is by no means unique. Satisfactory fits can also be obtained by employing a Fröhlich boxlike distribution [13] with the edge frequencies still given by Eqs. (4) and (5), in which case the evaluation of $\nu(\delta, T)$ from Eq. (1) can be done analytically. This clearly suggests that it is the asymmetric behavior of f_1 and f_2, and not so much the actual shape of $g(\ln f)$, which is responsible for the asymmetric features of the frequency-temperature plots in Fig. 2. If, for example, one assumes a Vogel-Fulcher scaling of all relaxation frequencies, $f = f_0\exp[-U/(T - T_0)]$, the curves at different δ values become nearly parallel and asymptotically diverge at the same temperature T_0, in disagreement with experiment.

The present picture has two major advantages. First, it clearly indicates the divergence of the lower boundary of the relaxation spectrum without the need for any crucial assumptions about the shape of the relaxation spectrum or, in fact, any model at all. Second, only the real part of the complex dielectric constant is involved, which can be measured much more accurately, especially at extremely low frequencies. Thus the data obtained at low temperatures, where the relaxation process starts to escape out of the experimental frequency window and which cannot be analyzed accurately enough in the Cole-Cole picture, are still useful in the δ picture, so that the experimental temperature interval has been effectively extended.

The parameter ε_s appearing in Eq. (1) represents the low frequency limit of the real part of the dielectric constant and is essentially obtained by extrapolating the measured values of $\varepsilon'(\nu)$ to zero frequency. This seems to imply that the analysis strongly depends on the shape of the distribution function through the parameters ε_∞ and ε_s; however, this is not the case for the following two reasons. First, ε_∞ can be measured directly and very precisely at high frequencies below 70 K where it is essentially temperature independent. Second, and perhaps even more important, ε_s is independently known from static experiments. To illustrate this point, in Fig. 3 the values of ε_s are plotted (crosses) versus the temperature down to 50 K. It can easily be seen that ε_s has precisely the same temperature dependence as the field-cooled static dielectric constant obtained in earlier charge monitoring experiments [2]. Above 50 K, the field-cooled and zero-field-cooled static susceptibilities, $\varepsilon_{\mathrm{FC}}$ and $\varepsilon_{\mathrm{ZFC}}$, respectively, were found to be equal on the experimental time scale. The experimental time scale of a zero-field-cooling experiment $t_{\exp}$ is determined by the longest time in which the polarization charge is allowed to build up after switching on the field, i.e., $t_{\exp} \approx 3000$ s at low temperatures. Also shown in Fig. 3 are the data for the field-cooled dielectric constant $\varepsilon_{\mathrm{FC}}$ [2] (full circles) below

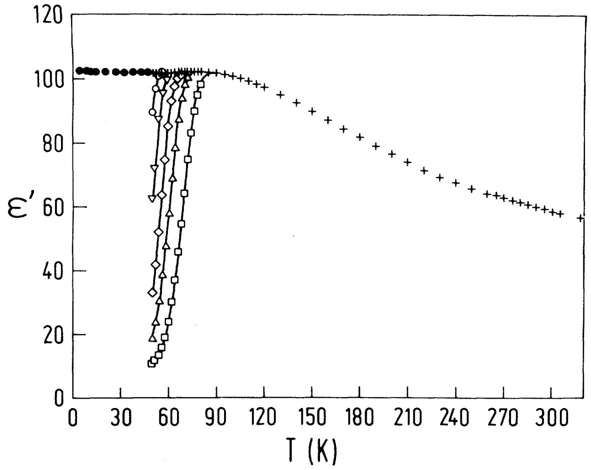

FIG. 3. Temperature dependence of the parameter ε_s (+) obtained from Eq. (1) and the field-cooled static dielectric constant $\varepsilon_{\mathrm{FC}}$ (●) from Ref. [2]. Also shown is $\varepsilon'(\nu, T)$ at various frequencies ν: 500 kHz (□), 10 kHz (△), 324 Hz (◇), 1 Hz (▽), 1 mHz (○).

50 K. The corresponding freezing temperature T_f, which may be defined as the point where the splitting between $\varepsilon_{\rm FC}$ and $\varepsilon_{\rm ZFC}$ occurs, must therefore lie in the region below 50 K for the above time scale.

Returning to the case of a dielectric relaxation experiment, we conclude that the time scale is here essentially determined by the measuring frequency, i.e., $t_{\rm exp} \approx 1/\nu$. To illustrate how this time scale affects the behavior of the low frequency dielectric constant, we have plotted in Fig. 3 the real part $\varepsilon'(\nu, T)$ for five different values of ν. It seems natural to associate the points where $\varepsilon'(\nu, T)$ starts to differ from the "true" static dielectric constant with the freezing temperature $T_f(t_{\rm exp})$, namely, the temperature where the splitting between $\varepsilon_{\rm FC}$ and $\varepsilon_{\rm ZFC}$ would occur in a field-cooling experiment on the same time scale. One may then argue that $T_f(t_{\rm exp})$ marks the point where the measuring frequency starts to exceed the lowest relaxation frequency, i.e., $\nu \geq f_1$. Thus, since $\tau_{\rm max} = 1/2\pi f_1$ diverges as $T \rightarrow T_0$, we realize that T_0 corresponds to $T_f(\infty)$, i.e., the "static" or equilibrium value of the freezing temperature, which would in principle be observable only in a static experiment on an infinite time scale.

It should again be stressed that the present study emphasizes the need for a dynamic description of the freezing process in deuteron glasses and related systems. Although static microscopic models have been useful for the discussion of NMR and other experiments carried out at temperatures above T_f, their extension to dynamic problems is far from trivial in view of the breaking of ergodicity which occurs at the glass transition. One may wonder in this context why the conventional static description of the freezing transition, according to which the spin glass order parameter $q(T)$ is zero above the freezing temperature T_f and nonzero below, could not be applied here. The point is that in deuteron glasses and related systems, $q(T)$ is always nonzero due to the presence of random fields [8]. Rather than rely on some model-dependent arguments to obtain an alternative static definition of T_f [2,9], we have adopted here the phenomenological concept of a dynamic ergodic-nonergodic spin glass transition [12]. Actually, phenomenological models based on hierarchically constrained dynamics do correctly capture many of the features of glassy relaxation [3]. In particular, the relaxation is predicted to occur over many time scales with the maximum relaxation time $\tau_{\rm max}$ diverging according to the Vogel-Fulcher law. Furthermore, the time dependence of the dielectric relaxation function is predicted to be of the Kohlrausch-Williams-Watts (KWW) form, i.e., $\Phi(t) = \exp[-(t/\tau)^\beta]$, and thus $\varepsilon^*(\nu) = \varepsilon_\infty - (\varepsilon_s - \varepsilon_\infty) \int_0^\infty dt \exp(-i\nu t)\, d\Phi/dt$. An expression of this type has recently been applied to a proton glass [14]. In the present case, however, it turns out that the KWW function gives a satisfactory fit only at temperatures above 100 K. As the temperature is lowered, the asymmetry predicted by the KWW law does not match the data, i.e., the low frequency side of the Cole-Cole diagram in Fig. 1 would increase very steeply, contrary to observation (cf. Ref. [7]).

In conclusion, the method of data analysis suggested in the present work provides a powerful tool to determine the behavior of the edge frequencies of the relaxation spectrum close to the freezing transition in deuteron glasses. Though the present empirical model may be regarded as perfectly general, it does not provide insight into the microscopic mechanism of glassy relaxation since the appropriate theoretical model of relaxation phenomena in complex systems is still missing. Formally, our results seem to lend support to the theory of hierarchically constrained dynamics. In particular, they give clear evidence that the maximum time scale diverges according to the Vogel-Fulcher law as one approaches the freezing transition; however, the relaxation function cannot be described by the KWW stretched exponential form favored by most dynamical models. Thus a need emerges for alternative phenomenological expressions describing the relaxation function in the time domain, and moreover, for appropriate dynamic models capable of explaining the observed relaxation behavior.

This work was supported by the Research Council of Slovenia. Special thanks are due to the Alexander von Humboldt Stiftung for donating the measuring equipment.

[1] E. Courtens, Phys. Rev. B **33**, 2975 (1986).

[2] A. Levstik, C. Filipič, Z. Kutnjak, I. Levstik, R. Pirc, B. Tadić, and R. Blinc, Phys. Rev. Lett. **66**, 2368 (1991).

[3] R. G. Palmer, D. L. Stein, E. Abrahams, and P. W. Anderson, Phys. Rev. Lett. **53**, 958 (1984).

[4] E. Courtens and H. Vogt, Z. Phys. B **62**, 143 (1986).

[5] E. Courtens, J. Phys. (Paris), Lett. **43**, L199 (1982); see also V. H. Schmidt, Jpn. J. Appl. Phys. Suppl. **24**, 944 (1985).

[6] Ping He, J. Phys. Soc. Jpn. **60**, 313 (1991).

[7] Z. Kutnjak, A. Levstik, C. Filipič, R. Pirc, B. Tadić, R. Blinc, H. Kabelka, A. Fuith, and H. Warhanek, J. Phys.: Condens. Matter **3**, 91 (1991).

[8] R. Pirc, B. Tadić, and R. Blinc, Phys. Rev. B **36**, 8607 (1987).

[9] R. Blinc, J. Dolinšek, R. Pirc, B. Tadić, B. Zalar, R. Kind, and O. Liechti, Phys. Rev. Lett. **63**, 2248 (1989).

[10] A similar behavior was observed earlier on the undeuterated RADP by H. J. Brückner, E. Courtens, and H.-G. Unruh, Z. Phys. B **73**, 337 (1988).

[11] M. V. Feigel'man and L. B. Ioffe, J. Phys. (Paris), Lett. **46**, L695 (1985).

[12] V. S. Dotsenko, M. V. Feigel'man, and L. B. Ioffe, *Spin Glasses and Related Problems*, Soviet Scientific Reviews Section A Physics Vol. 15, edited by I. M. Khalatnikov (Harwood, Chur, New York, 1990), p. 1.

[13] H. Fröhlich, *Theory of Dielectrics: Dielectric Constant and Dielectric Loss*, Monographs on the Physics and Chemistry of Materials Vol. 42 (Oxford Science Publications, Oxford, 1986), 2nd ed.

[14] S. L. Hutton, I. Fehst, R. Böhmer, M. Braune, B. Mertz, P. Lunkenheimer, and A. Loidl, Phys. Rev. Lett. **66**, 1990 (1991).